Rheology and Tube Model Theory of Bimodal Blends of Star Polymer Melts

B. Blottière,*,† T. C. B. McLeish,† A. Hakiki,‡ R. N. Young,‡ and S. T. Milner§

IRC in Polymer Science and Technology, Department of Physics and Astronomy, University of Leeds, Leeds LS2 9JT, England, Department of Chemistry, University of Sheffield, Sheffield S3 7HF, England, and Exxon Research and Engineering Company, Route 22 East, Annandale, New Jersey 08801

Received January 23, 1998; Revised Manuscript Received June 25, 1998

ABSTRACT: Experiments on solution-cast blends of two anionically synthesized monodisperse star-shaped polyisoprene molecules of widely different molecular weight exhibit a very rich rheological behavior. The time-dependent moduli are exponentially dependent on the relative volume fraction of each species. This work models these new features by extending existing theories for monodisperse melt of star polymers to the blend of two monodisperse star polymers with different molecular weight, keeping the same chemistry. The theory is based on the tube model with constraint release for star polymers in both an approximate and then a more exact level. The latter, with its treatment of nonactivated as well as activated breathing modes, is able to account quantitatively for the huge range of blend rheologies. With no extra parameters, it is able to account qualitatively for relaxation times and entire relaxation functions that vary over many orders of magnitude on blending.

1. Introduction

The theory of the tube model[1−3] first introduced for concentrated solutions and melts of linear polymers has been very successful in describing complex viscoelastic behavior. The main relaxation processes for such melts occur via tube length fluctuation and at lower frequencies by reptation. The reptation relaxation process describes the motion of the linear molecule along the length of its tube contour. This enables the molecule to escape its original tube to explore new paths. This tube concept was also applied to branched polymers and has been particularly successful. Branched polymers with a range of architectures have been studied in both monodisperse and polydisperse (commercial LDPE) form.[4] The simplest branched molecule is the one having a single branch point linking together three or more linear molecules having the same molecular weight. Such a branched molecule is called a star-shaped polymer molecule or star polymer. The main difference from linear polymers is the existence of the branch point. This will disallow the reptation of one arm of the molecule along its own tube, because the branch point acts like a pinning point for the entire molecule. Consequently the rheological properties of branched structures are significantly different from those of linear polymer melts.[5]

Although the relaxation by reptation is almost suppressed, the star molecule can still relax via arm fluctuations.[6] The free end of the arm can retract along its own tube and then explore a new path by extending back in another direction. This constrained diffusion of the free end of one arm is modeled as a particle moving through a potential well $U(s)$, where s measures the distance of retraction along the tube. The retraction therefore can be seen as an activated process with a defined attempt frequency which derives from the lowest Rouse mode of the arm. $U(s)$ is itself calculated from the energy of chain configuration.[8] Because each segment of the arm will have a different relaxation time that is exponentially dependent on the distance from the free end, the segments near the free end relax their stress by renewing configuration much faster than the ones near the core. Then the fast segments of the molecule are acting as solvent for the slow segments at the longer time scales associated with the with the slow segments' stress relaxation. This is called the dynamic dilution[9] model of constraint release. In the monodisperse case it works very well.[10]

For linear polymer melts, the constraint release is harder to treat because of the less well-separated relaxation times, and therefore it needs more sophisticated models to treat it.[11]

Because most applications are blends or polydisperse systems and often have both polydispersity in the molecular weight distribution and a mixing of random polymeric branched structures, it is of importance to understand the rheological properties of blends. The first step in studying and understanding the behavior of such complex polymeric liquids is to focus our attention on the simplest one. The simplest blended system where reptation does not occur is a blend composed of two monodisperse star-shaped molecules. The two molecules share the same chemistry but they each have a different and well defined molecular weight. Conversely, the question for any molecular model is: "Can this model be extended to polydisperse systems and blends?". Indeed blends are a hard test. For example blends of linear molecules and stars molecules are extremely complex because linear polymers can still reptate. We will see that star−star blends give an enormous range of rheological response. This work may also be regarded as step along the way toward developing and verifying rheological models for melts of different topology. It is very difficult to ascertain the topological structure of a melt (number and location of

* To whom correspondence should be addressed. E-mail: phybb@irc.leeds.ac.uk.
† University of Leeds.
‡ University of Sheffield.
§ Exxon Research and Engineering Co.

10.1021/ma980093t CCC: $15.00
Published on Web 12/09/1998

branches) by any existing experimental probes. Rheological response is, however, quite sensitive to even small amounts of branching. Comparing measured rheology to that predicted for an assumed branching structure could be a very useful characterization tool, if some rheological models for a rich enough set of branching structures were available.

In the extension of the models from the monodisperse to the blend case, the question of the mutual dependence of the time scale for each species is important. Simple mixing laws for the modulus such as the relation in (1),

$$G(t) = (\phi_1(G_1(t))^{1/\nu} + \phi_2(G_2(t))^{1/\nu})^{\nu} \qquad (1)$$

where ν is an arbitrary number,[12] are not expected to work in general because they assume time scales are not mutually affected by blending. This may be disguised in some cases by preexisting polydispersity on the blend fractions[13] but should find monodisperse blends a harder test. Indeed, we will find that no mixing law that assumes the relaxation times of the two species to be constant can work, because those relaxation times are observed to vary dramatically as blend fractions are varied. The relaxation times of the star arms depend on the dynamics entangling environment, which in turn depends on the degree of blending.

Limited data on star−star blends (η_0 and J_e^0 as functions of composition) have been published,[14] but not at the level of entire relaxation spectra. However, recent work on monodisperse melt blends has shown how critical the shape of the relaxation modulus is in testing a theory.[10,15,16]

The first part of this paper will describe the chemistry and synthesis of the star-shaped polyisoprene molecules as well as the rheological measurement. There follows the theoretical section that deals with the blend of star polymers first using the approximate constraint release model[9] and then using a more refined model that allows us to have access to the prefactors and Rouse regimes[10] in the calculation of the complex moduli G' and G''. We conclude with a few remarks and possible extension of our work. A control blend of a three-arm stars containing 10% of "two-arm" contaminant was made using precursor (arm) material of 95k.

2. Experimental Section

Synthesis. Benzene was distilled from sodium−potassium alloy on to solvent-free *n*-butyllithium and allowed to stand for several hours before distilling into the reactor. Methyltrichlorosilane was purified by distillation on the vacuum line and dissolved in benzene. *sec*-Butyllithium was distilled under high vacuum on to a coldfinger in a short path length apparatus and dissolved in benzene. The concentrations of the solutions of $MeSiCl_3$ and *sec*-BuLi were determined by hydrolysis and titration and appropriate quantities were ampoulised. Triethylamine was stored over sodium−potassium alloy. Isoprene was treated with dibutylmagnesium for at least 12 h then distilled onto *n*-BuLi and kept at −10 °C for an hour before distilling into the reactor. Polymerization of the isoprene was initiated by benzene by *sec*-BuLi and was allowed to proceed for 24 h to ensure complete reaction and the chains were then capped by the addition of some 5 units of butadiene. A small sample was withdrawn and analyzed by SEC using a Waters 150 instrument calibrated with a set of Polymer Laboratories polyisoprene standards. $MeSiCl_3$ was introduced to the reactor in an amount such that there was a ratio of living polymer:$MeSiCl_3$ = 3.1:1, and reaction was allowed to continue for several days before methanol was added to terminate the small excess of living polymer. The star polymers were purified by fractional precipitation from 1% solutions in toluene by the addition of methanol. SEC was used to monitor the progress of the fractionation.

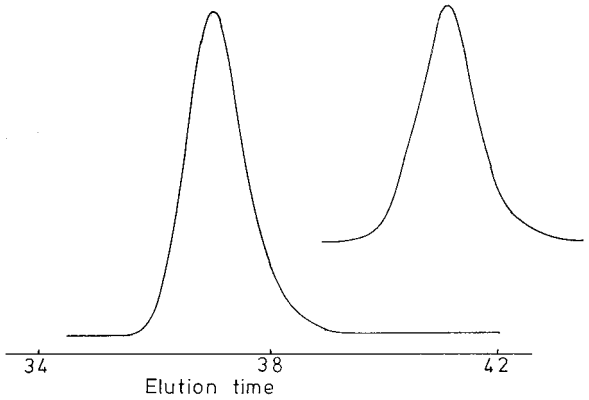

Figure 1. SEC chromatograms of parent arm M = 144 000 (upper trace) and, after fractionation, the resulting three-armed star (lower trace). Time axis is in min.

SEC analysis showed that the arms and the three armed stars derived from them had narrow molecular weight distributions (M_w/M_n = 1.02) and that fractionation had successfully removed the excess unlinked arm. Figure 1 shows the chromatograms for the higher molecular weight arm and resulting star: those for the lower molecular weight pair were entirely analogous. The elution times for the stars corresponded to the anticipated molecular weights when allowance was made for their architecture,[17] and there was no evidence for the presence of any coupled arm contaminants. The GPC trace of this blend gave a noticeably wider peak than either of the single-component materials used in this study. Additional confirmation of the molecular weights and monodispersity was made by multiangle light scattering attached to the GPC column. Anticipated and measured molecular weights were within experimental uncertainties of 28 000 and 144 000 for the lower and higher molecular weight three-arm stars respectively.

Rheology. Rheological experiments were made on a Rheometrics RDAII rheometer in oscillatory mode. Frequency sweeps from 10^{-2} to 10^2 rad·s^{-1} at temperature from 25 to 120 °C were time−temperature superimposed using WLF parameters for polyisoprene. Strains were everywhere within the regime of linear response.

Other data from experimental rheology of star polyisoprene molecules are available from ref 5 in the monodisperse case showing a broad range of rheological behavior. The binary polymeric blends we have modeled here are composed of star-shaped polyisoprene whose arm molecular weights are, respectively, 28 000 and 144 000.

As shown by data for monodisperse melts of star polymers in Figure 2, the rheology is extremely sensitive to the molecular weight: the bigger the molecule is the wider the spectrum of the relaxation time function. Indeed for the unblended star of the higher molecular weight, our data do not quite reach the terminal zone even at the highest temperatures and the longest experimental times consistent with the stability of the

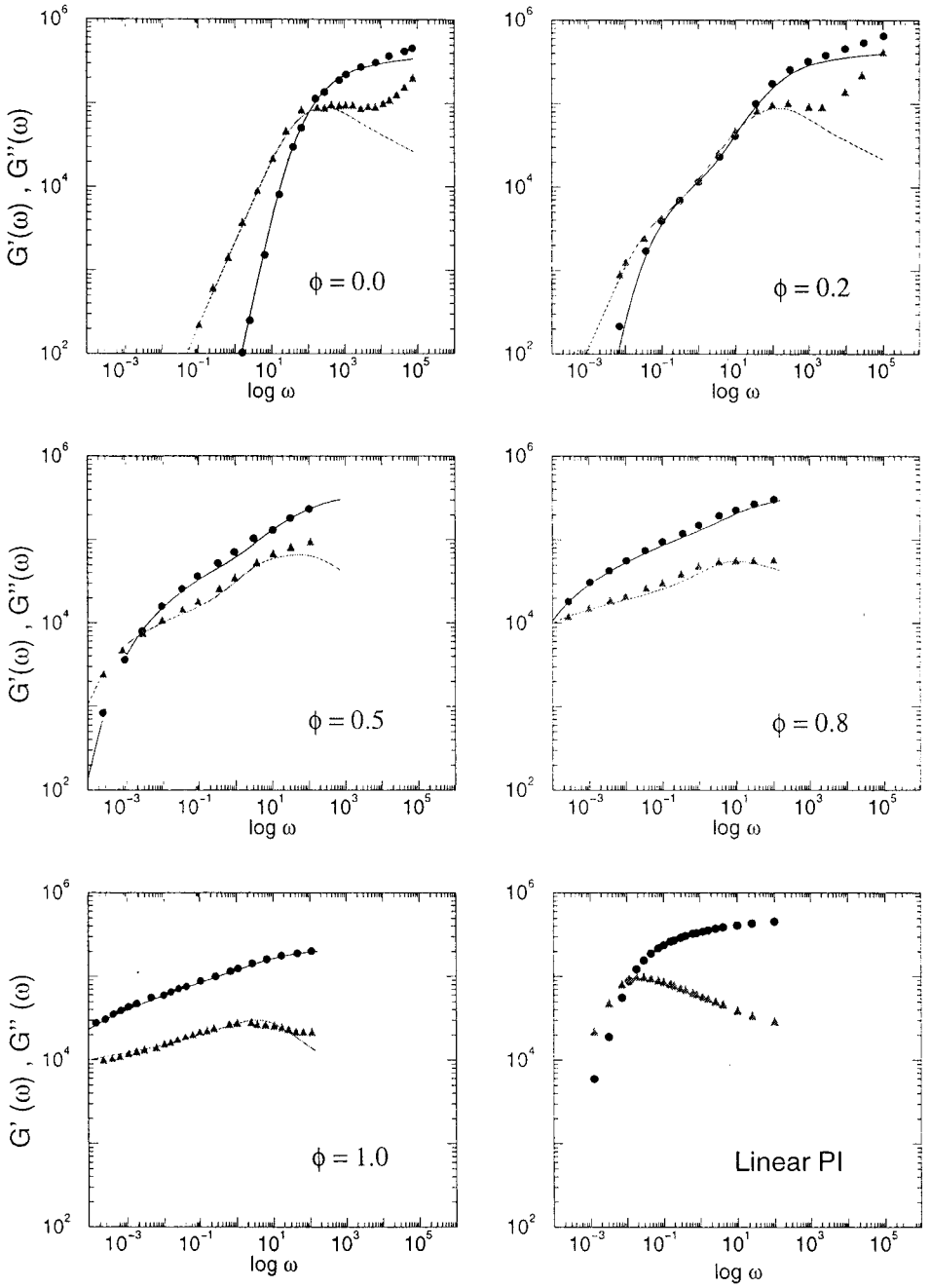

Figure 2. Experimental data on star melt: $M_1 = 28\,000$ monodisperse (top left); $M_2 = 144\,000$ monodisperse (bottom left). Blends: 20/80 (top right), 50/50 (center left), 80/20 (center right). Bottom right: linear polyisoprene $M = 475\,000$.

sample. We also include rheology on a high molecular weight (475k) monodisperse linear PI for comparison (see Figure 2). As previously reported,[5] the spectra of the star polymers is quite different in nature from the nearly single mode from of the linear material. This arises directly from the different mechanism of stress relaxation (arm fluctuation vs reptation). When blending these two star-shaped molecules with such different relaxation spectra, the rheology exhibits a new qualitative behavior at each composition, especially for blends whose composition contains a majority of low molecular weight star. Indeed, from the blend data shown in Figure 2, the most striking qualitative shape of G' and G'' appears for the blend which contains 20% of the high molecular weight star. For such blends, G' and G'' are closely interlaced and exhibit a "double hump".

The data also clearly show that relaxation time scales themselves are strong function of composition. The 80/20 blend, for example, has a terminal time which is far greater than that of the monodisperse melt of low molecular weight star and simultaneously much smaller than that of the high molecular weight star melt. So even for this simple sort of blend, phenomena arise showing that dynamic interactions between the two species cannot be ignored.

3. Theory

In this section we briefly review essential prerequisites of the theoretical development in the following section. Following initial treatments of entangled arm fluctuation,[6,7] Pearson and Helfand[8] have calculated the resulting relaxation spectrum in the case of a star polymer molecule relaxing in a fixed network. Retrac-

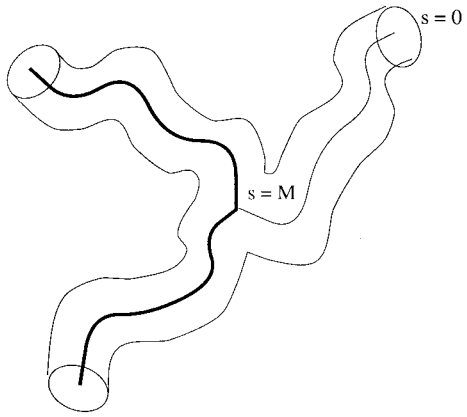

Figure 3. Star polymer and its tube: curvilinear coordinate *s*.

tions of the free end along a tube distance *s* occur in an effective potential well $U(s)$. In a fixed network $U(s)$ is quadratic in *s*. In consequence the relaxation time $\tau(s)$ for the segment at *s* grows exponentially with the square of the distance to the free end for a star-shaped molecule. The model was later extended in an approximate way to melts of star polymer molecules[9] and showed in this case that the potential has a cubic correction induced by the dynamic dilution of constraints. Recent improvements[10] calculated the prefactor for $\tau(s) \approx \exp(U(s))$, and allowed for rapid processes near the free end. We first recall the main results for these theories in the monodisperse case. Then we extend these models to the blend case.

A. Retraction Potentials. The main relaxation process in a melt of monodisperse star-shaped polymer molecules occurs via arm retraction (see Figure 3). These dynamics occur in an effective free energy potential which conveys an exponential dependence on the curvilinear coordinate *s* of the relaxation time function $\tau(s)$. Because of this exponential dependence, each tube segment has its own relaxation time and will relax more or less rapidly depending on its distance from the free end. It is then obvious that the faster segments will not constrain at all the movement of the very slow segments standing near the branch point, and therefore, the former will act then as solvent for the slower one. This is what is meant by dynamic dilution.

First, we review the calculation in the simplified problem where dynamic dilution is not taken into account: the free end retracting into its tube is modeled as a particle moving through an harmonic potential well. Solving the modified first time passage time problem for the free end moving through a potential well $U(s)$ in an approximate way, leads to the following result for the relaxation time of the arm:

$$\frac{\mathrm{d}\tau(s)}{\mathrm{d}s} = \tau(s)\frac{\partial U(s)}{\partial s} = \frac{2\nu}{M_e}\left(\frac{s}{M}\right)\tau(s) \tag{2}$$

The physical motivation for this approach is the imposition of Boltzmann weight $e^{\Delta U}$ for an incremental retraction Δs, for which a typical waiting time is $\tau(s)$. The solution to (2) is

$$\tau(s) = \tau_0 \exp\left\{\frac{U(s)}{k_B T}\right\} \tag{3}$$

where τ_0 is an "attempt-time" for arm retractions. At an approximate level, τ_0 was to be taken as constant, though this is not a necessary condition (see section 3B).

The potential well is then the path length free energy potential scaling as the square of the distance. This comes from the rubber-elastic entropic constraints on the chain given the position of its free end:[9]

$$U(s) = \frac{k_B T \nu}{M_{e0} M} + \text{constant} \tag{4}$$

The curvilinear coordinate s measures the tube length from the free end to the branch point and ranges from 0 to *M*, the molecular weight of the arm. M_{e0} is the entanglement molecular weight. The parameter ν comes from the tube model and is equal to $^{15}/_{8}$.[9] We call $U(s)$ the "bare potential" as it will be modified when applying the constraint release hypothesis.

The key assumption of the dynamic dilution hypothesis for the relaxing arms is to modify the bare potential as the entanglement molecular weight varies at the local level as

$$M_e(s) = \left(1 - \frac{s}{M}\right)^{-\alpha} M_{e0} \tag{5}$$

The exact choice of α depends on the concentration-scaling of the entanglement molecular weight (and hence G_0). The "naive" value of α is $\alpha = 1$, which results from arguing that the arc-length between entanglements along a chain in a network diluted by a factor of ϕ scales as $1/\phi$. Experimental values of alpha obtained from the plateau modulus of theta solutions as a function of concentration suggest $\alpha = {}^{4}/_{3}$, which is in agreement with a subtle scaling argument of Colby and Rubinstein.[20] However, in ref 10, it is found that taking $\alpha = 1$ results in acceptable descriptions of rheological data if one takes a value of M_{e0} some 20% too large. For simplicity, we follow this approach here. Replacing expression 5 into the differential equation (2) for the time relaxation function leads to a new expression:

$$\tau(s) = \tau_0 \exp\left[\frac{2\nu}{M_{e0}M}\left(\frac{s^2}{2} - \frac{s^3}{3M}\right)\right] \tag{6}$$

Therefore the new effective potential has a cubic correction:

$$U_{\text{eff}}(s) = \frac{2\nu k_B T}{M_{e0}M}\left(\frac{s^2}{2} - \frac{s^3}{3M}\right) \tag{7}$$

When one is calculating the terminal time for both expressions 3 and 6, the constraint release calculation reduces the value of $U_{\text{eff}}(M)$ by a factor of 3.

$\tau(M)$ is therefore reduced by a very large factor of $\exp(^{2}/_{3}\nu M/M_e)$. This factor is then transmitted through the viscosity η_0 by the relaxation modulus $G(t)$ as it depends on the relaxation time function $\tau(s)$

$$\eta_0 = \int_0^\infty G(t)\,\mathrm{d}t \tag{8}$$

with

$$G(t) = \int_0^M \mathrm{d}s\,\frac{\partial G(\Phi(s))}{\partial s}\exp(-t/\tau(s)) \tag{9}$$

where $\Phi(s) = 1 - s/M$ is the entangled volume fraction for monodisperse stars.

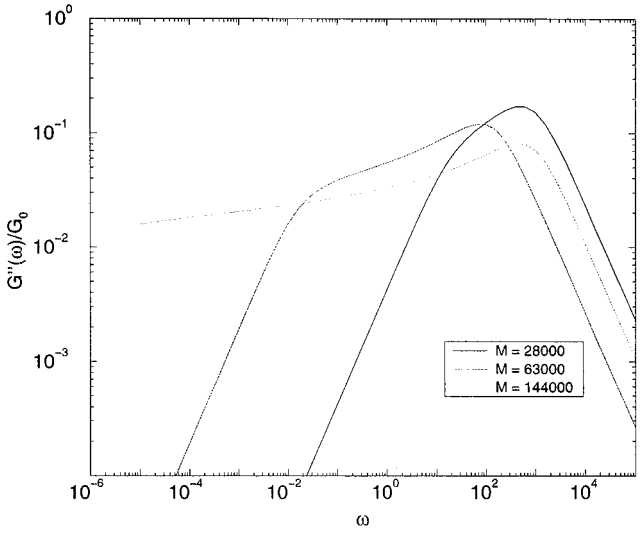

Figure 4. Computation of $G''(\omega)$ for three different values for the molecular weight of arm M_a = 28 000, 63 000, and 144 000 and a value of M_e = 4000, representative of PI, using the no prefactor model.

It is simple to derive analogous expressions for $G'(\omega)$ and $G''(\omega)$, the storage and loss moduli—as the real and imaginary parts of the complex modulus $G^*(\omega)$:

$$G^*(\omega) = 2G_0\int_0^M (1 - s/M)\frac{i\omega\tau(s)}{1 - i\omega\tau(s)}\,ds \qquad (10)$$

In the monodisperse case as shown in Figure 4, the loss modulus for star polymers shows a wide range of relaxation times.

B. Prefactors for $\tau(s)$ and Fast Processes. A recent work,[10] which we will require, takes into account two main features that allow a fully quantitative account of the entangled dynamics of star polymers: first we have to consider that for small s, whenever $U_{eff}(s) \ll k_BT$, arm retraction is not activated and it is rather the fast Rouse-like diffusive motion of the free end along the tube that controls the tube-segment relaxation times; second we will have access to the prefactor of the exponential term by calculating the first passage time for a diffusing free end to retract to a length s, the effective potential being given.

When the potential $U_{eff}(s)$ is much smaller than k_BT then the part of the molecule that fulfils this condition is not conditioned by this potential but will freely diffuse via the curvilinear superposition of Rouse modes of the chain. This occurs only near the free end, because the large free energy for deep retractions strongly favors the lowest Rouse mode there. The early fast diffusion movement of a small fractional distance x of the free end leads to the following expression for its relaxation time function, where $x = s/M$ is the normalized curvilinear coordinate (ranging from 0 to 1):

$$\tau_e(x) = \frac{225\pi^3}{256}\left(\frac{M}{M_e}\right)^4 \tau_0 x^4 \qquad (11)$$

The form of this relation arises from the non-Fickian monomeric Rouse diffusion: $x(t) \propto t^{1/4}$. For the other parts of the molecule that do not fulfill the above condition, the arm retraction is activated. Solving the first time passage problem for the free end to retract to a deep segmental position x gives the following expression for the activated relaxation time function with its prefactor:

$$\tau_a(x) = \frac{L^2}{D_{eff}}\frac{\exp(U_{eff}(x))}{[(U'_{eff}(x))^2 + 2U''_{eff}(1)/\pi]^{1/2}}\left(\frac{\pi}{2U''_{eff}(0)}\right)^{1/2} \qquad (12)$$

The coefficients L and D_{eff} are respectively the path length of the arm and the effective curvilinear diffusion constant of the free end and are related to τ_0, the Rouse time for an entanglement length as mentioned below in relation 33.

Putting together the expression for the two relaxation functions $\tau_e(x)$ and $\tau_a(x)$ in a crossover formula leads to

$$\tau(x) \approx \frac{\tau_e(x)}{e^{-U_{eff}(x)} + \tau_e(x)/\tau_a(x)} \qquad (13)$$

Relation 13 is substituted into the expression of $G(t)$ which remains unmodified from (9). The application of this approach to the two monodisperse components of the blend series is given in Figure 2.

C. How to Treat Star Blends. The case of blends is a hard test for these models of entangled branched melts. The blend of our experiments is composed with two polymer star-shaped molecules having the same monomeric chemistry, but differing only in their total molecular weight. The large one is more than 5 times larger than the small one. For such a blend, we do not expect a simple mixing law because time scales for relaxation of the two components are mutually affected in a very strong manner. The system has a different time scale for each species of star polymer molecule driven by a differential equation analogous to eq 3

$$\frac{d\tau_i(s_i)}{ds_i} = \tau_i(s_i)\frac{2\nu}{M_e}c(s_i)\frac{s_i}{M_i}, \quad i = 1,2 \qquad (14)$$

where $c(s_i)$ is the concentration of material (from both components) that is not relaxed at the time $\tau_i(s)$. Clearly the functions $\tau_i(s)$ will depend on the arm molecular weight, M_i. Let introduce $z = s_i/M_i^{1/2}$, $s_i \in [0, M_i]$—we find this is the coordinate for relaxation which is universal among stars of different arm molecular weight because it eliminates all dependence on the molecular weight as seen below in (15)—the transformed version of (14) for any i. Then $\tau(z)$ is universal: it obeys a differential equation independent of M.

$$\frac{d\tau(z)}{dz} = \tau(z)\frac{2\nu}{M_e}c(z)\,z \qquad (15)$$

The concentration function of the melt, $c(z)$, depends on the molecular weights of each species, but it now is reduced to one universal arc length coordinate

$$c(z) = 1 - \left(\frac{s_1}{M_1}\phi_1 + \frac{s_2}{M_2}\phi_2\right) \qquad (16)$$

$$c(z) = 1 - \left(\frac{\phi_1}{\sqrt{M_1}} + \frac{\phi_2}{\sqrt{M_2}}\right)z, \quad z \le \sqrt{M_1} \qquad (17)$$

Here without loss of generality $M_1 < M_2$. For $z > \sqrt{M_1}$, all parts of the smaller star have relaxed, so changes to the entanglement network arise only via the relaxation in M_2. So the effective concentration of unrelaxed segments after the smaller star has com-

pletely relaxed has the following form:

$$c(z) = 1 - \phi_1 - \frac{\phi_2}{\sqrt{M_2}}z, \quad \sqrt{M_1} < z \le \sqrt{M_2} \quad (18)$$

Therefore we have two domains, which we refer to as α and β for the differential equation to solve, describing the evolution of the relaxation time function $\tau(z)$:

$$\alpha: \quad \frac{\tau'_\alpha(z)}{\tau_\alpha(z)} = \frac{2\nu}{M_e}\left[1 - \left(\frac{\phi_1}{\sqrt{M_1}} + \frac{\phi_2}{\sqrt{M_2}}\right)z\right]z, \quad z \le \sqrt{M_1} \quad (19)$$

$$\beta: \quad \frac{\tau'_\beta(z)}{\tau_\beta(z)} = \frac{2\nu}{M_e}\left[1 - \phi_1 - \frac{\phi_2}{\sqrt{M_2}}z\right]z, \quad \sqrt{M_1} < z \le \sqrt{M_2} \quad (20)$$

The two domains connect via the mutual boundary condition $\tau_1(\sqrt{M_1}) = \tau_2(\sqrt{M_1})$. This leads to the following results for the final expressions of $\tau(z)$ at the level of the effective potential. The exponential coefficient in expression 22 is due to boundary condition of $\tau(z)$ at $z = \sqrt{M_1}$; for $z \le \sqrt{M_1}$

$$\tau_\alpha(z) = \tau_0 \exp\left\{\frac{2\nu}{M_e}\left[\frac{z^2}{2} - \left(\frac{\phi_1}{\sqrt{M_1}} + \frac{\phi_2}{\sqrt{M_2}}\right)\frac{z^3}{3}\right]\right\} \quad (21)$$

and for $\sqrt{M_1} < z \le \sqrt{M_2}$

$$\tau_\beta(z) = \tau_0 \exp\left(\frac{\nu\phi_1 M_1}{3M_e}\right)\exp\left\{\frac{2\nu}{M_e}\left[(1-\phi_1)\frac{z^2}{2} - \frac{\phi_2}{\sqrt{M_2}}\frac{z^3}{3}\right]\right\} \quad (22)$$

After all expressions were retransformedin order to get functions depending on x only (x ranging from 0 to 1), we introduce now this new expression for τ_α and τ_β into the expression of $G(t)$ via the contribution of each star. To avoid any confusion in our notation, we introduce new labeling for the concentration function and the time relaxation function: the first subscript notation refers to the species, rather than the domain of solutions of the differential equation. Let us use the subscript label "1" for the smaller star and the subscript label "2" for the larger molecule. The problem that arises concerns only the large molecule as the concentration function and the relaxation time function split over the domain of solutions. Therefore we add this second subscript to that which this indicates on which domain the functions apply: "α" and "β". For the same reason, the integral corresponding to contributions from the larger star splits into two parts as the concentration function does so as seen above:

$$\frac{G(t)}{G_0} = 2\phi_1\int_0^1 c(x_1)e^{-t/\tau(x_1)}\,dx_1 + 2\phi_2\int_0^1 c(x_2)e^{-t/\tau(x_2)}\,dx_2 \quad (23)$$

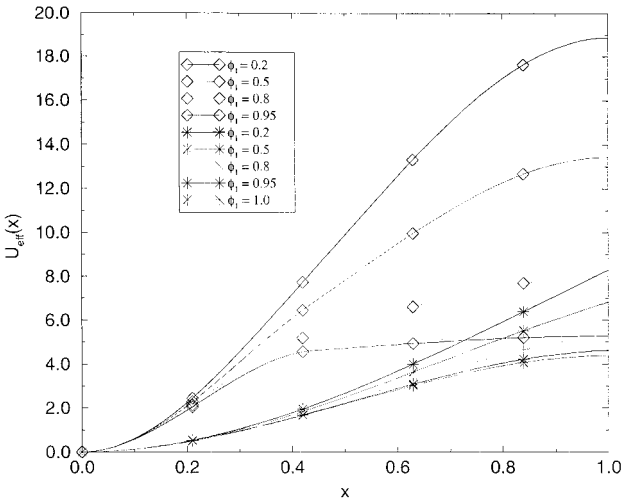

Figure 5. Effective potential of the big star (diamond curves) and small star (star curves) for different values of the volume fraction ϕ_1 of the small star, using the no prefactor approximate model extended to the blend.

This leads to the following expressions for the rigidity and loss moduli

$$\frac{G'(\omega)}{G_0} = 2\phi_1\int_0^1 c_1(x)\frac{\omega^2\tau_1(x)}{1+\omega^2\tau_1{}^2(x)}\,dx + 2\phi_2\int_0^{\sqrt{M_1/M_2}} c_{2\alpha}(x)\frac{\omega^2\tau_{2\alpha}(x)}{1+\omega^2\tau_{2\alpha}{}^2(x)}\,dx + 2\phi_2\int_{\sqrt{M_1/M_2}}^1 c_{2\beta}(x)\frac{\omega^2\tau_{2\beta}(x)}{1+\omega^2\tau_{2\beta}{}^2(x)}\,dx \quad (24)$$

$$\frac{G''(\omega)}{G_0} = 2\phi_1\int_0^1 c_1(x)\frac{\omega\tau_1(x)}{1+\omega^2\tau_1{}^2(x)}\,dx + 2\phi_2\int_0^{\sqrt{M_1/M_2}} c_{2\alpha}(x)\frac{\omega\tau_{2\alpha}(x)}{1+\omega^2\tau_{2\alpha}{}^2(x)}\,dx + 2\phi_2\int_{\sqrt{M_1/M_2}}^1 c_{2\beta}(x)\frac{\omega\tau_{2\beta}(x)}{1+\omega^2\tau_{2\beta}{}^2(x)}\,dx \quad (25)$$

The prefactors to expressions for the relaxation time spectrum require for our system the form of $U_{eff}(x)$ for each component. As for the case of monodisperse stars, this is implied by the solutions for $\tau(s)$ in relations 21 and 22. So we may write

$$U_{\text{eff }1}(x) = \frac{2\nu M_1}{M_e}\left[\frac{x^2}{2} - \left(\phi_1 + \phi_2\sqrt{\frac{M_1}{M_2}}\right)\frac{x^3}{3}\right] \quad (26)$$

$$U_{\text{eff }2,\alpha}(x) = \frac{2\nu M_2}{M_e}\left[\frac{x^2}{2} - \left(\phi_2 + \phi_1\sqrt{\frac{M_2}{M_1}}\right)\frac{x^3}{3}\right] \quad (27)$$

$$U_{\text{eff }2,\beta}(x) = \frac{2\nu M_2\phi_2}{M_e}\left[\frac{x^2}{2} - \frac{x^3}{3}\right] + \frac{\nu M_1\phi_1}{3M_e} \quad (28)$$

Figure 5 displays the effective potential of the small

and large star molecules. We will discuss later on in the next section all implications for such curves.

Now let us focus on the fast diffusion of the free end. In the monodisperse case we have seen that the characteristic times are given by relation 11. In a blend of two monodisperse singly branched polymers this leads to the two characteristic time functions for each species:

$$\tau_{e,1}(x) = \frac{225\pi^3}{256}\left(\frac{M_1}{M_e}\right)^4 \tau_0 x^4 \tag{29}$$

$$\tau_{e,2}(x) = \frac{225\pi^3}{256}\left(\frac{M_2}{M_e}\right)^4 \tau_0 x^4 \tag{30}$$

Now the first passage time may be considered: the general form of (12) requires the first and second derivative of the potential functions in order to obtain the prefactor in the expressions of the activated relaxation time functions. Finally, the crossover formula 13 of the early diffusion relaxation time function and the activated relaxation time function will be substitute in the expression of $G'(\omega)$ and $G''(\omega)$. In the next section we compare this calculation with the experimental data and discuss the results we have obtained, for the potential functions, the time scales, and the moduli.

4. Discussion

This section is devoted to the analysis of the expressions for the relaxation moduli 24 and 25 that we obtained for the binary blend of stars. The moduli are built from the entropic potential functions 26−28, which enter the time relaxation functions. The time scale enters also the moduli expression via the prefactors of the relaxation functions $\tau(x)$ which are given by relations 21 and 22. We restrict our discussion to the ratio of molecular weights represented by the data. Other choices do not alter the qualitative behavior.

Potential. The potential functions are a fruitful source of insight into the dynamic interaction of the two components. A first look at the potential curves for the small star and for the large star (Figure 5) shows for both molecular species a strong dependence on the blend composition.

For the small stars, as ϕ_1 decreases from 1 to 0, the potential increases but with a drastic change in its shape: at $\phi_1 = 1.0$, the well-known dynamic dilution shape is recovered for the potential, but as the density of small star decreases, the potential curve tend to an asymptotic harmonic curve. We will comment on this further below. The final value of the potential, i.e., for $x = 1.0$, is almost doubled going from 4.3 ($\phi_1 = 1.0$) to 8.3 ($\phi_1 = 0.2$).

This effect is even greater for the large molecule: at $x = 1.0$, the value of the potential is 5.2 for $\phi_1 = 0.95$ and equals to 18.8 for $\phi_1 = 0.2$. For high values of ϕ_1, the shape of the potential is highly altered: there is a strong "knee" at a well-defined value around $x = \sqrt{M_1/M_2}$. This corresponds to the point at which the smaller stars complete their relaxation. Beyond this point, the potential is flattened by the diluting effect of the small molecules. This means that the large molecule can retract its arms more easily inside their tubes than at lower values of ϕ_1 and, of course, than in the pure dynamic dilution case. The small molecules" help" the large ones to relax by softening their potential.

On the other hand, the large molecules have an enhancing effect on the potential for the smaller ones. In the limit of small ϕ_1, the presence of much larger stars in majority is nearly equivalent to a fixed network, thus taking the effective potential from the dynamic dilution[9] to the fixed network[8] result.

The very first conclusion we can draw is that the large molecules are more strongly affected, qualitatively and quantitatively, by the blend composition than the small ones. The dynamic dilution is enhanced for the large stars when ϕ_1 increases. The small stars behave differently: at low concentrations they behave like a star in a fixed network, and at higher concentrations they retrieve the melt behavior. This conclusion is remarkable in that, for blends of star polymers, the relaxation time spectrum is much narrower in width than a naive superposition of relaxation components would predict. The cooperative dynamics induce exponentially strong motional "narrowing".

Time Scales. The great advantage of working at the level of prefactors to the exponential of $\tau(x)$, that enables us to ascribe a magnitude to the time scale of molecule motions. Transposed to the blended case, it allows us to differentiate between the two molecular species in the melt as they have different terminal relaxation times.

The constant parameters in relations 11 and 12, respectively, τ_0, L^2, and D_{eff}, are not independent of each other. First, let us recall their definitions: L is the length of one arm, D_{eff} is the diffusion coefficient of one arm, and τ_0 is the relaxation time for an entanglement length. This constants can be expressed by molecular parameters such as the monomer friction coefficient ζ, the monomer length b, the number of monomers N_i of the species "i" and the number of monomers between entanglements N_e:

$$\frac{L_i^2}{D_{eff}} = \frac{5\zeta N_i^3 b^2}{8k_B T N_e} \tag{31}$$

Similarly, τ_0 has an expression using the same molecular parameters

$$\tau_0 = \frac{\zeta N_e^2 b^2}{3\pi^2 k_B T} \tag{32}$$

Clearly, these two relations are linked by

$$\frac{L_i^2}{D_{eff}} = \tau_0 \frac{15\pi^2}{8}\left(\frac{N_i}{N_e}\right)^3 \tag{33}$$

From the previous relation, it can be established that the ratio L_1^2/D_{eff} over L_2^2/D_{eff} of prefactors scales as $(N_1/N_2)^3$. This will have a great impact on the moduli, as it will shift the components of each species for G' and G'' away from each other. Combining this term with those arising from derivatives of $U_{eff}(x)$ leads to a final dependence of the prefactor on molecular weight of $(N_1/N_2)^{3/2}$.

Moduli. Having focused our attention on the potentials and the time scales in the above paragraphs, we can turn now to the fundamental functions that are the moduli. We will first briefly compare our two models with the data.

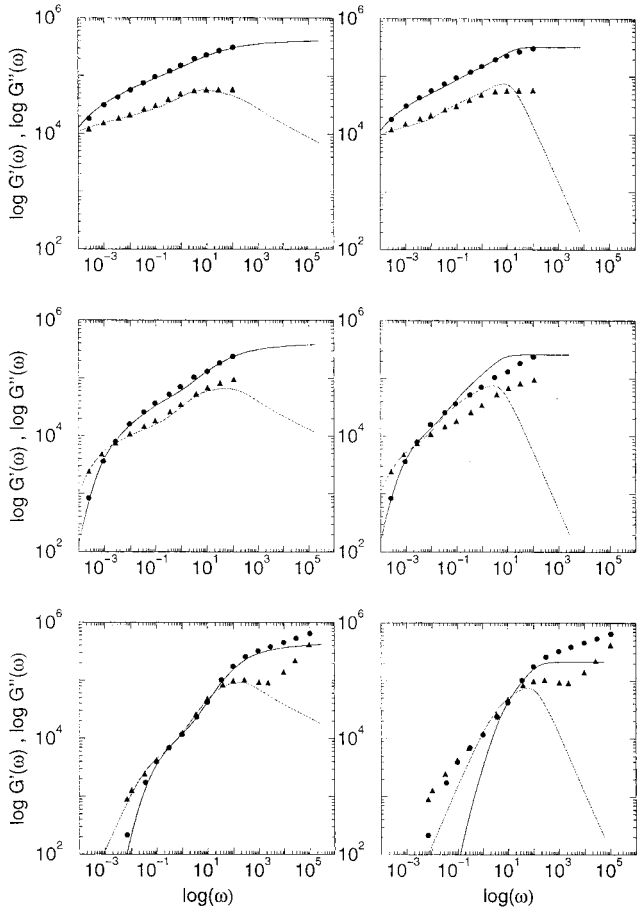

Figure 6. Left: full tube blend model (lines) and experiments (circles G' and triangles G''). Right: no prefactor approximate blend model (lines). From top to bottom, the blends are composed as follows: 20/80, 50/50, and 80/20 (small molecule/large molecule). $M_1 = 28\,000$, $M_2 = 144\,000$, and $M_e = 5500$.

Figure 6 shows the plots of $G'(\omega)$ and $G''(\omega)$ for the model with and without calculation of prefactors. Both levels of modeling predict the moduli very well in the 20/80 case. However the prefactor-level model begins to do rather better in the 50/50 case, and does spectacularly well in predicting the unusual shape of the two rheological functions in the 80/20 blend while the single-exponential approximation fails rather seriously. This situation contrasts with that of monodisperse star melts, in which the prefactors make a much smaller correction to the predicted forms of $G^*(\omega)$. In the following we use only the full version of the model. The theory predicts the entire relaxation spectra with no extra parameters for the widely ranging functions in the middle of the composition range, even though time scales range over many orders of magnitude.

From the moduli expressions we have obtained previously, (24) and (25), we can extract the contribution of each species; that includes the effect of the other species. Graph 7 shows such a decomposition for G'' for $\phi_1 = 0.2$ and $\phi_1 = 0.8$: $G'' = G''_1 + G''_2$. For a low value of ϕ_1, the majoritory contribution to G'' comes from the large stars over a wide frequency range (around 6 decades), and the contribution of the small molecule becomes more important at high frequencies over only $2^1/_2$ decades and is about the same order of magnitude. When ϕ_1 is close to 0.8 the contributions of the two species are more well balanced: still at low frequencies, the main contribution is due to large molecules ($3^1/_2$ decades) but is soon balanced by the small molecules at high frequencies where the small molecules are dominate over more than 5 decades. Comparison of the results of our calculations for $\phi_1 = 0.2$ and $\phi_1 = 0.8$ indicates that the contribution of the small star in both cases has the same intensity at low frequencies up to $\omega \sim 1$, when they alone contribute. At higher frequencies, the contribution is of course more important when the small stars are more numerous. Comparing now the contribution of the large stars at the two previous values of ϕ_1 gives another picture: over the whole frequency spectrum, the contribution of the large star is lowered drastically for $\phi_1 = 0.2$.

Table 1

blend composition	$10^5\tau_0$	$10^{-5}G_0$, N·m^{-2}
0/100	2.0	2.30
20/80	1.4	4.11
50/50	2.5	4.11
80/20	1.6	4.52
100/0	1.1	4.11

The effect of the two different time scales can be then understood from the fact that a large value for the prefactor time constant, depending on the molecular weight, shifts the moduli curves toward the low frequencies, and conversely a small value the prefactor shifts the moduli curves toward the high frequencies. This time scale ratio is drastically affected by the "dynamic dilution" of the large stars by the small. When adding the two shifted curves, it leads to the double hump shape and interlacement of G' and G'' over 2 decades in frequency range in the 80/20 blend when the contributions of the two species have the same order of magnitude at $\omega \sim 1$.

Parameters and Comparison to Data. The blends of our experiments consist purely of polyisoprene molecules. The small molecule has an arm molecular weight of $M_1 = 28\,000$, whereas the large one has an arm molecular weight of $M_2 = 144\,000$. The molecular weight of isoprene is $M_0 = 68$. Our calculations do imply also two other fundamental molecular parameters that are the friction coefficient ζ and the monomer length b. Accepted values for these two parameters can be found in the literature: $\log \zeta = -6.41$ cgs unit from Ferry[18] and $b \approx 6.35$ Å from Fetters.[19] From relation 32, we can then calculate a value for $\tau_0 = 8.4 \times 10^{-6}$ s, at 25 °C, which is used in our computations. This gives us a very good value for the fastest relaxation time in the system. Nevertheless we will have to adjust the value of τ_0 slightly, as a free parameter, to fit our calculations with the data; we have use also a value for $M_e = 5500$. This order-one adjustment seems to be commonly required when comparing linear and star melts.[10] In Table 1, we give the values for τ_0 and G_0 we obtained to fit the theoretical curves with experimental ones.

We can also compare the experimental values for G_0 with a theoretical value which is given by

$$G_0 = \frac{\rho RT}{M_e} = 4.11 \times 10^5 \text{ N·m}^{-2} \qquad (34)$$

The coefficient L_i^2/D_{eff} scales as N_i^3, the number of monomers in the molecule; then it differs for the two stars: for the small star $L_1^2/D_{eff} = 0.02$ s, and for the big star $L_2^2/D_{eff} = 2.80$ s. The ratio of the large star time over the small star time is around 136. This clear separation of time scales is further (and much more significantly) amplified by the exponential factors in the

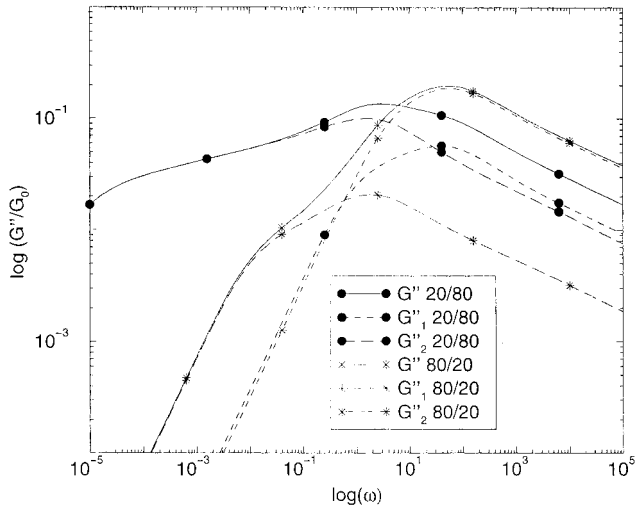

Figure 7. Full tube blend model: relative component of M_1 and M_2 in $G''(\omega)$. 20/80 blend.

expression for relaxation times, (22). This will introduce two different time scales in our expression of G' and G''. As we have seen (Figure 6), using these values into our model gives a good agreement with experimental data except in the 80/20 and to some extent the 50/50 case when using the exponential term only; the calculation of prefactors to $\tau(s)$ enhances considerably the fit for these blend compositions. Nevertheless, we have to adjust slightly these curves with the data by tuning the two free parameters G_0 and τ_0 for each blend. For each blend, we have a different set of adjusting parameters, though these lie within typical experimental errors in torque and temperature control in the rheological experiments.

As we can see in the above expressions for the storage and loss moduli, we can identify two regimes that can be seen most clearly in the 80/20 blend: in the first regime, the two entangled molecules start to relax until the time needed for the small one to have completely relaxed. During the second regime the long molecules complete their relaxation.

Blending Rule. The longest relaxation time in the blend $\tau_{2\ \mathrm{blend}}$ is given by relation 22 when $x_2 = z_2/\sqrt{M_2} = 1$. By using the approximate relation 6, it can be shown that

$$\tau_{2\ \mathrm{blend}} = \tau_1^{\phi_1}\tau_2^{\phi_2} \tag{35}$$

where τ_1 and τ_2 refer to the pure component longest relaxation time. But it should be noted that this rule is only true at the constant prefactor approximate model level. Similar relationships for the viscosity have been proposed empirically.[14]

Viscosity and Compliance. Previously published viscoelastic data on a star−star blend[14] can be compared to this model. (We evaluate the predictions for η_0 and J_e^0 using Graessley and Struglinski data because their lower degree of entanglement permitted complete access to the terminal relaxation regime.) Figure 8 displays experimental curves (circles) of viscosity η_0 and equilibrium recoverable compliance J_e^0 for a binary blend of three-arm star polybutadiene molecules with arm molecular weights equal respectively to 25 000 and 42 333 from ref 14. The full prefactor level model is used

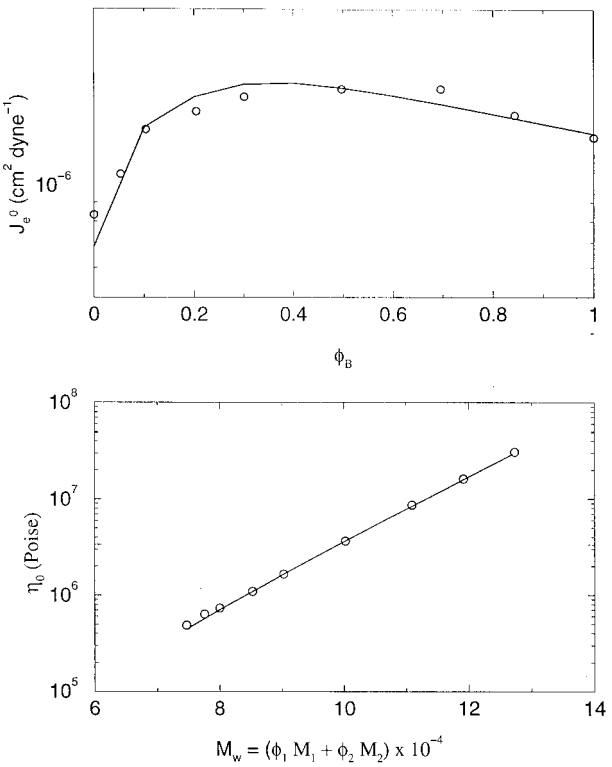

Figure 8. Compliance and viscosity for a binary mixture of three-arm star polybutadiene molecules: circle, experiment; line, theory. $M_1 = 25\,000$, $M_2 = 42\,333$, and $M_e = 2900$. Experimental data are from ref 14.

to compute η_0 and J_e^0 via the standard relations:

$$\eta_0 = \int_0^\infty G(t)\,\mathrm{d}t = 2G_0\int_0^1 (1-x)\,\tau(x)\,\mathrm{d}x \tag{36}$$

$$J_e^0 = \frac{1}{\eta_0^2}\int_0^\infty t\,G(t)\,\mathrm{d}t = \frac{2G_0}{\eta_0^2}\int_0^1 (1-x)\,\tau^2(x)\,\mathrm{d}x \tag{37}$$

Figure 8 shows a good agreement between the model (lines) and experimental data used in the calculation, $M_1 = 25\,000$ and $M_2 = 42\,333$ for the arm molecular weights. To compensate for the choice of $\alpha = 1$ in relation 5, we have used a higher value of the molecular entanglement weight than can be found in the literature:[21] $M_e = 2900$. This higher value of the entanglement molecular weight is consistent with the value obtained with the linear−star blend as well as the one with have used for the star−star polyisoprene blend above. In reference,[14] in order to fit the viscosity data with a basic star theory the authors have used the following expression:

$$\eta_0 = 1.47 \times 10^3 \exp(\mathrm{M}/12900) \tag{38}$$

where $M = 3M_a$ and M is replaced by $\bar{M}_w = \phi_1 M_1 + \phi_2 M_2$.[22] The factor of 12 900 in the exponential term in the above expression seems to correspond to a value of $M_e = 2700$. Our value is slightly bigger due to the molecular weight dependence of the prefactor as $M^{3/2}$, for which the choice of M_e in relation 38 has to compensate. The fitting both qualitatively and quantitatively of η_0 and J_e^0 from previous data supports the accurate fitting of the terminal zone of our own data. This suggests that the present level of tube model for

star polymers is accurate across the entire spectrum of entangled modes including the terminal zone.

5. Conclusions

The picture is now the following for binary blends of star-shaped molecules. First of all, the dynamic blending is extremely sensitive to the relative composition of the melt. On one hand we may have small stars moving through a relatively fixed network of large stars and we retrieve the result of Pearson and Helfand. On the other hand, the small molecules help the big ones to relax faster by diluting their network. Two régimes are identified: first both molecules start to relax together with mutual effect. Then when the small molecule has finished relaxing, the only remaining molecules to relax are the big ones, which entangle only with each other. The cooperative effect gives a strong "motional narrowing" to the time scales.

Where entangled dynamics dominate, our model and calculations give good agreement with the experiments. This is true over a wide range of relaxation spectrum, and the terminal zone in particular. In this case of blends, the refinements of the prefactor model are absolutely necessary to treat the data quantitatively. This is in contrast to monodisperse stars, for which the no prefactor approximation is less unacceptable. We can see also that the relaxation times in branched polymer blends are extremely sensitive to blending, typically carrying an exponential dependence on ϕ.

Finally we conclude that the "dynamic dilution" tube theory for constraint release in star polymer melts passes the very severe test imposed by the system of star−star blends, supporting further development of the theory to more complex systems. The remarkable result of this work is that, with no extra parameters, the tube model is able to account qualitatively for relaxation functions that vary orders of magnitude on blending.

Acknowledgment. We gratefully acknowledge the Smith and Nephew Group Research Centre and the University of Leeds sponsoring a CASE studentship for this work.

References and Notes

(1) de Gennes, P.-G. *Scaling Concept in Polymer Physics*; Cornell University Press: Ithaca, NY, 1979.

(2) Doi, M.; Edwards, S. F. *The Theory of Polymer Dynamics*; Clarendon Press: Oxford, England, 1986.

(3) Doi, M. *Introduction to Polymer Physics*; Clarendon Press: Oxford, England, 1996.

(4) McLeish, T. C. B. *Rheology of Entangled Polymers: Topological and Nonlinear Effects*: *Theoretical Challenges in the Dynamics of Complex Fluids*; NATO ASI Series 339; Kluwer: Dordrecht, The Netherlands, 1997; pp 87−114.

(5) Fetters, L. J.; Kiss, A. D.; Pearson, D. S.; Quack, G. F.; Vitus, F. J. *Macromolecules* **1993**, *26*, 647−654.

(6) Doi, M.; Kuzuu, N. Y. *J. Polym. Sci., Polym. Lett. Ed.* **1980**, *18*, 775−780.

(7) de Gennes, P.-G. *J. Phys. (Paris)* **1975**, *36*, 1199.

(8) Pearson, D. S.; Helfand, E. *Macromolecules* **1984**, *17*, 888−895.

(9) Ball, R. C.; McLeish, T. C. B. *Macromolecules* **1989**, *22*, 1911−1913.

(10) Milner, S. T.; McLeish, T. C. B. *Macromolecules* **1997**, *30*, 2159−2166.

(11) Rubinstein, M. *Theoretical Challenges in Polymer Dynamics*: *Theoretical Challenges in the Dynamics of Complex Fluids*, NATO ASI Series 339; Kluwer: Dordrecht, The Netherlands, 1997; pp 21−52.

(12) Groves, D. J.; McLeish, T. C. B.; Chohan, R. K.; Coates, P. D. *Rheol. Acta* **1996**, *35*, 481−493.

(13) Groves, D. J.; McLeish, T. C. B.; Ward, N. J.; Johnson, A. F. *Polymer* **1998**, *39*, 16, 3877−3881.

(14) Struglinski, M. J.; Graessley, W. W.; Fetters, L. J. *Macromolecules* **1988**, *21*, 3, 783−789.

(15) Milner, S. T.; McLeish, T. C. B. Submitted for publication in *Macromolecules*, 1998.

(16) Hakiki, A.; Young, R.; Johnson, A. J.; Milner, S. T.; McLeish, T. C. B. Submitted for publication in *Macromolecules*, 1998.

(17) Bauer B. J.; Fetters L. J. *Rubber Chem. Technol.* **1978**, *51*, 406.

(18) Ferry, J. D. *Viscoelastic Properties of Polymers*; Wiley: New York, 1980.

(19) Fetters, L. J.; Hadjichristidis, N.; Lindner, J. S.; Mays, J. W. *J. Phys. Chem. Ref. Data* **1994**, *23*, 619−640.

(20) Colby, R. H.; Rubinstein, M. *Macromolecules* **1990**, *23*, 2753−2757.

(21) For polybutadiene, ref 18 gives $M_e = 1850$.

(22) Due to a different notation convention, in ref 14, M_1 and M_2 refer to the molecular weight of the whole molecule.

MA980093T